Future Journal of Pharmaceutical Sciences

RESEARCH

Open Access

Efficient in vitro oxaliplatin delivery with functionalized single-walled carbon nanotube for enhanced colon cancer treatment

Dheeraj S. Randive[1], Kiran P. Shejawal[1], Somnath D. Bhinge[2], Mangesh A. Bhutkar[1], Namdeo R. Jadhav[3], Sandeep B. Patil[4] and Sameer J. Nadaf[5*]

Abstract

Background Site-specific transport of medicinal products to malignant cells and tissues is an intriguing area since it has an ability to safeguard healthy cells. Selective upregulation of folate receptors on colon cancer cells is usual. Consequently, folate receptors have become one of extensively studied target moieties for targeting the delivery of chemotherapeutics. Hence, the study aimed to anchor folic acid, chitosan and oxaliplatin to the functionalized nanotube (FA-CHI-FSWCNT-OXA) for targeting folate receptors on colon cancer cells. The purification process of single-walled carbon nanotubes (SWCNTs) involved the use of an ultrasonic-assisted acid digestion method. The developed complex was evaluated using FTIR, DSC, SEM, XRD and in vitro dissolution studies. SRB and MTT assays were used to assess in vitro cytotoxicity of oxaliplatin and FA-CHI-FSWCNT-OXA) against HT29 and COLO320DM cell lines. Further, progression of apoptosis in cells was investigated using flow cytometry.

Results The FTIR results corroborated drug attachment over carbon nanotube (CNT), whereas the TEM results validated the nanosizing (1–300 nm) of the developed system. Drug entrapment in CNT was found to be 93.43 ± 1.65%, and in vitro drug release was found to be 94.73 ± 0.90% after 24 h. The complex reduced viability of 92.35 ± 0.942% cells than oxaliplatin's 66.58 ± 0.38% inhibition, revealed by MTT assay. In the SRB assay, the developed system showed 91.22 ± 0.90% inhibition, whereas oxaliplatin showed 76.69 ± 0.52% inhibition against HT29 cells.

Conclusions Conclusively, the developed system exhibited better cytotoxicity effects as compared with plain oxaliplatin. Our findings are suggestive of the potential development of CNT-anchored antineoplastic agents for target-specific delivery.

Keywords Carbon nanotube, Oxaliplatin, Colon cancer, Cytotoxicity, Apoptosis

*Correspondence:
Sameer J. Nadaf
sam.nadaf@rediffmail.com
[1] Department of Pharmaceutics, Rajarambapu College of Pharmacy, Kasegaon, Maharashtra 415404, India
[2] Department of Chemistry, Rajarambapu College of Pharmacy, Kasegaon, Maharashtra 415404, India
[3] Krishna Vishwa Vidyapeeth (Deemed to Be University), Krishna Institute of Pharmacy, Karad, Maharashtra 415110, India
[4] Department of Pharmacology, Dr. Shivajirao Kadam College of Pharmacy, Kasabe Digraj, Maharashtra 415311, India
[5] Department of Pharmaceutics, Bharati Vidyapeeth College of Pharmacy, Palus 416310, India

Background

Reportedly cancer is among the leading causes of death in the USA and even in most of the developed countries. Nearly 25% of deaths occur only due to cancer, which stands next to cardiovascular diseases. Among the internal malignancies, colonic cancer and cancer of the rectum are considered to be more frequent [1]. A large number of cases are reported for colorectal carcinoma (CRC), which has been demonstrated to be the third most common type of internal malignancy worldwide [2, 3]. CRC is classified into five stages based on

the degree of the depth of local invasion, metastasization, and lymph node involvement, with the earliest stage being stage 0 and stage IV being the advanced stage [4]. Prompt and effective management of CRC in general comprises the amalgamation of several characteristic strategies of oncology, i.e., chemotherapy, radiation and surgery. Several therapeutic strategies have proven their effectiveness in the treatment of colorectal cancer. However, effective treatment of metastatic disease remains out of reach for physicians due to a lack of effective drugs, and it has thus remained practically incurable [5].

Traditional drug delivery therapy is typically limited in their ability to function on the desired target. Also, owing to the lack of specificity of anticancer drugs to act on tumors or their inability to reach at site and act specifically on the target cell/tissue, they may produce undesirable side effect(s) that are not intended. Furthermore, in patients with metastasis from CRC, despite the use of targeted molecular therapies and standard chemotherapeutic regimens, the 5-year survival rate is less than 10%, due to associated lethal side effects on normal cells and emergence of multidrug resistance [6].

The European Union and several other countries' regulatory bodies have already approved the use of oxaliplatin as an anticancer agent to treat colorectal cancers [7]. Oxaliplatin, a platinum drug of the third generation, belongs to the 1,2-diaminocyclohexane family, which induces DNA cross-linking and initiates DNA double-strand breakage [8]. It is regarded as a prominent drug in effective treatment because it has ample beneficial effects, such as being less toxic and having relatively negligible oral and cross resistance when compared to its counterparts. Moreover, oxaliplatin exhibits a substantial antitumor effect and has proven effective in the treatment of CRC and its metastatic form [9–11]. However, oxaliplatin induces acute and chronic neuropathic pain, which leads medical professionals to lower dosages or stop therapy altogether. Oxaliplatin has recently been shown to have a capacity to change the genetic and epigenetic patterns of nerve cells [12, 13].

Hitherto, numerous studies have been conducted on the usage of various cutting-edge nanocarrier platforms to produce intended desired therapeutic effects. Nanocarriers, namely liposomes, nanostructured lipid carriers, polymeric nanoparticles, metal nanoparticles, magnetic nanoparticles, silica nanoparticles, solid lipid nanoparticles, and carbon nanotubes (CNTs), have been studied to promptly deliver chemotherapeutic(s) to the tumors with minimum toxic effects to the normal healthy cells [14, 15]. At the end of the twentieth century, following a significant progression, including the discovery of carbon nanotubes (CNTs), the scientific community was introduced to an entirely new set of possibilities for nanoscale study [16–18].

The development of a CNT-based novel drug delivery system could be efficient in delivering anti-cancer drugs at the target site [19, 20]. Moreover, CNTs offer better cell permeation and other physical properties as compared to other nanocarriers in novel drug delivery systems. CNTs have received a huge amount of attention in biomedical applications due to their large surface area, stability, high aspect ratio, and rich surface chemical functionalities. It has proven to be excellent transporters for drug and biomolecule delivery [21].

Single-walled carbon nanotubes (SWCNTs) or multi-walled carbon nanotubes (MWNTs) are the popular types of CNTs [22, 23]. However, due to their extreme low solubility, pristine SWCNTs fail to undergo prompt circulation in biological systems. Furthermore, low solubility hampers the entry of SWCNTs to cells via endocytosis. Nevertheless, the utility of SWCNTs may be improved by modifying their surface properties to impart enhanced hydrophilicity, which in turn facilitates better interaction and effective binding of several drug substances. Through suitable functionalization, CNTs have been employed as nanocarriers to carry anticancer medicines [24], genes, and proteins for chemotherapy. They have also been utilized as mediators for photothermal treatment (PTT) and photodynamic therapy (PDT) for the direct elimination of cancer cells [25–27]. Owing to their greater surface area, CNTs possess the ability to adsorb or undergo conjugation with diverse therapeutic moieties [28].

Folate receptor (R-FR) and its substrate folic acid (FA) are just two of the many receptors that can indicate cancer. They possess an ability to act specifically on cancer cells by interacting with membrane-anchored proteins of these cells. In several types of human cancers, namely lung, breast, colon, and renal, R-FR is found to be over expressed, the maximum being observed (> 90%). This has resulted in the use of FA as a vital ligand to achieve target specificity for anti-cancer agents and other diagnostics [29].

Therefore, in the current research, SWCNTs have been subjected to acid functionalization to attach the carboxylic groups on their surfaces. For effective encapsulation of SWCNTs, chitosan, a biopolymer obtained from a natural source, has been successfully tried, also in aqueous conditions. Owing to its hydrophilic nature and cationic charge, it is known to augment the stability profile of nanoparticles (NPs) [29–32]. Additionally, chitosan exhibits important features such as its positive charge, which provides a suitable means for electrostatic interaction, which rules out the necessity of chemical binding with NPs [33–36].

Therefore, the intent of the present work was to overcome the shortcomings of systemic administration of oxaliplatin by use of functionalized SWCNTs which will help to protect the healthy cells upon their exposure to the drug.

Methods

The SWCNTs, having a diameter of 1–2 nm, a purity of > 90%, and a length of > 50 mm, were procured from AD Nanotechnology, Bengaluru, India. Chitosan (min 70%, $(C_6H_{11}NO_4)_n$), folic acid (MW 441.4 g mol^{-1}), oxaliplatin (MW 397.3 g mol^{-1}), N, N-(3-dimethylaminopropyl)-N′-ethyl carbodiimide hydrochloride (EDC. HCl) (MW 191.7 g mol^{-1}), nitric acid, and sulfuric acid were purchased from Research laboratories, Mumbai, India. The other chemicals used in the experimental work were of AR grade.

Purification and functionalization of single-walled CNTs

The purification process of single-walled carbon CNTs involved the use of an ultrasonic-assisted acid digestion method [37]. Initially, 0.5 g of single-walled CNTs underwent bath sonication in a 100 mL solution of 0.5 M HNO_3, with this treatment lasting for 0.5 h. Subsequently, the single-walled CNTs were refluxed at 120 °C for a 24 h duration. Afterward, the solution underwent filtration, and the resulting material was rinsed with distilled water until the pH of the filtrate became neutral. The cleaned SWCNTs then underwent an additional 0.5 h bath sonication in water and were subsequently dried at 100 °C for 12 h. This purification process yielded a thin, black mat comprising purified SWCNTs.

Furthermore, SWCNTs were functionalized with briefly, 120 mL of a solution containing 96% H_2SO_4 and 70% HNO_3 (v/v = 3:1) were taken in a beaker. Then, 30 mg of SWCNTs were added to it. At 80 °C for about 16 h, the mixture was then subjected to ultrasonic irradiation. Further, it was filtered, washed with the distilled water until a pH of 7.0 was reached, and finally dried in a vacuum to obtain functionalized SWCNTs (FSWCNTs) [38–40].

Preparation of chitosan-loaded system CHI-FSWCNTs

To enhance the aqueous solubility of modified COOH-SWCNTs, we employed chitosan, a biopolymer, by subjecting 20 mg of functionalized COOH-SWCNTs to ultra-sonication within a solution containing chitosan (40 mg) dissolved in 40 mL of 0.1 M aqueous sodium chloride for approximately 25 min as per procedure mentioned by Randive et al., 2023 [41]. Subsequently, the solution was maintained at room temperature and continuously stirred for 18 h using a magnetic stirrer. Chitosan in the free form was removed by washing the CHI-FSWCNTs using centrifugation for an 8000 rpm. CHI-FSWCNTs were then subjected to drying and stored properly.

Oxaliplatin loading to the CHI-FSWCNT

In the third step, 9 mg of oxaliplatin (OXA) and 3 mg of CHI-FSWCNTs were added to 6 mL of phosphate buffer solution (PBS) (pH 7.4) and stirred at ambient temperature for about 16 h. CHI-FSWCNT-OXA, thus obtained, was recovered by centrifugation with PBS until the supernatant liquid was colorless. The concentration of free drug (unbound) was measured spectrophotometrically at 520 nm.

Preparation of folic acid-loaded system CHI-FSWCNTs-OXA

The obtained CHI-FSWCNT-OXA (4 mg) in the aforesaid third step was suspended in a PBS buffer solution (8 mL; pH 7.4) containing folic acid (6 mg). 5 mg of 1-Ethyl-3-(3-dimethylaminopropyl) carbodiimide-HCl was added to facilitate solubilization of folic acid. The resulting mixture was allowed to stand at room temperature for approximately 16 h while being stirred. Finally, ultrapure was used to wash the obtained product a number of times so as to get rid of the unreacted substances. It was dried properly at ambient temperature to obtain the final nanosystem FA-CHI-FSWCNT-OXA [42].

Characterization of developed system

FTIR spectroscopy

FSWCNT, CHI-SWCNTs, OXA, and FA-CHI-FSWCNT-OXA nanocomposites were analyzed, and their spectra were determined using an FTIR spectrophotometer (Bruker Alpha Echo ATR) at the scanning range of 4,000–400 cm^{-1}.

SEM and TEM analysis

SEM (Schottky, SU5000) and TEM analysis were used to determine the structure of the SWCNT and FA-CHI-FSWCNT-OXA nanocomposites, following the loading of oxaliplatin.

X-ray diffraction (XRD)

XRD-6000, an X-ray diffractometer (Bruker: range: D8 discover), was used to determine the XRD patterns of FA-CHI-FSWCNT-OXA. The conditions are being maintained as follows: Range—2 h, Speed—4°/min at 10°—80°, Voltage—40 kV and 30 mA, and Radiation—Cu Kα within configurations of θ–2θ).

Zeta potential and particle size analysis

The HORIBA scientific Nanopartica SZ100 was used for the determination of the size of the particle and their zeta potential; the conditions being 30 °C and an angle

of detection of 90°, 0.1 mL of FA-CHI-FSWCNT-OXA 10 mg mL^{-1} was diluted to 10 mL with DMSO, 5 mL of this diluted sample was transferred to a cuvette, and the zeta potential was determined [43]. The particle size of the FA-CHI-FSWCNT-OXA composite was confirmed by a particle size analyzer.100 µL of FA-CHI-FSWCNT-OXA containing 10 mg/mL of composite was diluted with an appropriate volume of DMSO, and the particle size was measured.

Differential scanning calorimeter (DSC)

The changes in the relative specific heat associated with transitions in carbon NTs were recorded by DSC, which offers fruitful information related to physicochemical changes owing to exothermic as well as endothermic transitions, or any alteration in the heat capacity. Nanosystem FA-CHI-FSWCNT-OXA was characterized by the DSC analysis [44].

Thermo-gravimetric analysis (TGA)

Chemical as well as physical characters like sublimation, vaporization, absorption, adsorption, chemisorption, desorption, dehydration, redox reactions, and decomposition are obtained by TGA [45, 46]. The TGA graph represents the change in mass of carbon NTs as a function of time or temperature, indicating either a weight increase or decrease. Physicochemical properties of the FA-CHI-FSWCNT-OXA complex were characterized by the TGA.

Drug entrapment efficiency (EE)

Often, estimating drug EE involves quantifying the amount of drug present in CNTs, which was done using a method specified by Sobh et al. [47], wherein the amount of unloaded drug was determined in the clear supernatant of CNTs by centrifugation at 5000 rpm (30 min) which was then recorded as absorbance at 520 nm using an ultraviolet–visible spectrophotometer (Jasco V630, Japan). The standard plot for oxaliplatin was also determined. EE of oxaliplatin was estimated as per the equation stated below:

$$\mathrm{EE}(\%) = \frac{\text{The weight of drug entrapped in SWCNTs}}{\text{Intial weight of oxaliplatin}} \times 100 \quad (1)$$

In vitro drug release studies

The dialysis bag method was used to perform the in vitro drug release of oxaliplatin from FA-CHI-FSWCNT-OXA nanocomposites. The studies were carried out in a vessel that contained simulated intestinal fluid or simulated gastric fluid. Dialysis bags (Mol. Wt. cut-off 12 kDa, purchased from Sigma-Aldrich) were dipped in the buffer solution for equilibration before their use. In 3 mL of buffer saline, 500 mg of FA-CHI-FSWCNT-OXA nanocomposites were suspended, and then it was filled into the dialysis bag, which was suspended in the receptor compartment containing dissolution medium (50 mL). The media was kept closed and stirred at 100 rpm at 37 °C ± 0.5 °C temperature [32]. A sample (3 mL) was withdrawn at specific time intervals for analysis of the drug released from FA-CHI-FSWCNT-OXA nanocomposite, and every time a similar amount of buffer was replenished so as to keep up the sink conditions. The amount of drug released was noted spectrophotometrically at 520 nm [47].

Cytotoxicity assay

MTT assay

Dulbecco's modified Eagle's medium (DMEM) that has been fortified with 10% fetal bovine serum was used to preserve the COLO320DM and HT29 cell lines [45]. The cells were added to a 96-well plate at a density of 1×10^4cells mL^{-1} per well and cultured for 24 h at 37 °C. During incubation, the cells were consequently exposed to 100 µg mL^{-1} of the oxaliplatin as a standard and FA-CHI-FSWCNT-OXA. For 24 h, the plates were incubated, and then 10 µL of MTT (thiazolyl blue tetrazolium bromide) dye (5 mg mL^{-1} in phosphate-buffered saline) was added per well so as to measure the cell proliferation. Further, the plates were incubated for 4 h at a temperature of 37 °C in a humidified chamber containing 5% CO_2. It resulted in the formation of formazan crystals, owing to the reduction in dye by viable cells. The formed crystals in each well were dissolved by adding 200 µL of DMSO. The absorbance of the resulting solution was measured at 490 nm. The cytotoxicity of the compounds was determined using the following formula [45]:

$$\text{Percent cytotoxicity} = \frac{\text{Reading of control} - \text{Reading of trated cells}}{\text{Reading of control}} \times 100 \quad (2)$$

SRB assay

DMEM fortified with 10% fetal bovine serum was used to maintain human COLO 320 DM and HT29 cell lines. The cells were cultured at a density of 1×10^4 cells per well in a 96-well plate, solution was added, and the culture was incubated continuously for 24 h at 37 °C. Following that the cells were exposed to 100 µg mL^{-1} of oxaliplatin, FA-CHI-FSWCNT-OXA and standard. Thereafter, 50 µL TCA (50%) was added to each well separately, and the plate was kept at 4 °C for 1 h. The plates were then washed with TDW (triple-distilled water) and allowed to

air dry. Further, 100 µL SRB dye was added to each well and set aside for 30 min at room temperature. Lastly, the plates were washed three times with 1% acetic acid and allowed to air dry. Subsequently, 200 µL of tris buffer solution was used, and the absorbance was measured at 490 nm. The percent cytotoxicity exhibited by the compounds under study is calculated using Eq. (2) [48–53].

Apoptosis assay

Flow cytometry was used for the apoptosis study of the cancer cells using altered plasma membrane phospholipids filled with Annexin V-FITC (a lipid-loving dye). In a 24-well flat-bottom microplate equipped with cover slips, the selected cells were suspended. The cells were maintained in a CO_2 incubator at 37 °C for 12 h and washed repeatedly with PBS.

After washing the cells, they were centrifuged at 500×g for 5 min at 4 °C. The supernatant liquid was removed, and the obtained cell pellets were resuspended in ice-cold 1X binding buffer at 1×10^5 mL^{-1}, whereas the cold temperature was maintained by keeping the tubes in an ice bath. Thereafter, Annexin V-FITC (1 µL) and PI (5 µL) was added in each sample. All tubes were placed in an ice bath and incubated in the dark for 15 min. Finally, ice-cold 1X binding buffer (400 µL) was added and mixed gently, and labeled cells were analyzed immediately under flow cytometry with Cell Quest software (Becton Dickinson) [50].

Statistical analysis

GraphPad Prism 8 software (Windows 64-bit version 8.0.1) was used to analyze the statistical data obtained from the cytotoxicity studies. The results obtained after the performance of the tests were analyzed by one-way ANOVA with Dunnett's post-test analysis of variance. Mean ± SEM of all the calculated values was calculated. $P<0.05$, 0.01, or 0.001 were considered statistically significant. For the determination of the size of the prepared systems, ImageJ software (Java2HTML Version 1.5) was utilized.

Results

Purification, cutting, and functionalization of SWCNTs were carried out as per the reported procedure [45] with the intent to clear dirt and carbon-defective particles. The reported method was used to load oxaliplatin onto a FSWCNTs in the first step, confirmed by an FTIR study. In the second step, the chitosan was attached to the FSWCNTs for solubility and other advantages discussed in the introduction. Further, oxaliplatin was loaded to the CHI-FCNTs for therapeutic action as decided. In the last step, the folic acid was attached to the CHI-FSWCNT-OXA, for targeting specific cancer cells. Folic acid has an affinity for the folate receptor, which is overexpressed in colon cancer. Oxaliplatin was attached to the surface of FSWCNTs, along with folic acid and chitosan, which specifically target cancer cells in the colon [38, 39].

Characterization parameters

FTIR analysis

Oxaliplatin's IR spectrum showed weak peaks at 1656.36, 3207.17, 1069.09, 2883.36, 1219.88, 1254.27, and 1447.49 cm^{-1}, which corresponds to bond stretching of C=O, N–H, C–O, C–H, C–C, C–N, and CH_2 (scissor present in alkene group), respectively. Primary amines showed two peaks, namely $N–H_{symmetric}$ and $N–H_{asymmetric}$ at 3075.30 and 3154.45 cm^{-1}, respectively. Moreover, N–H wag and N–H bending were observed at 800.04 and 1601.56 cm^{-1}, respectively [44]. In the case of plain SWCNT, weak peaks at 834.99 and 1638.98 cm^{-1} were attributed to the stretching of the C=C bending and C–C in the alkene group, respectively [29]. After functionalization of SWCNTs, C=O (carbonyl), C–O and O–H (hydroxyl) bond stretching vibrations of the -COOH group were expected in the IR spectrum. The IR spectrum of FSWCNTs showed peaks for carbonyl, hydroxyl, and C-O groups at 1690.71, 3083.13, and 1185.25 cm^{-1}, respectively, which may confirm the functionalization of SWCNTs [29].

The IR spectrum of FA-CHI-FSWCNT-OXA retained the characteristic peaks of the hydroxyl group, C=O, N–H, C–O, C–H, C–C, C–N, and CH_2 (scissor) at 1606.78, 1024.87, 2859.27, 1151.18, 1209.70, and 1451.87 cm^{-1}, respectively. Moreover, $N–H_{symmetric}$ and $N–H_{asymmetric}$ were observed in the IR spectrum at 3113.34 and 3162.78 cm^{-1}. Also, N–H wag and N–H bending were observed at 802.14 and 1575.01 cm^{-1}, respectively. In the spectra of matrices combined with oxaliplatin (Fig. 1), signals corresponding to the drug were not observed, maybe due to its low concentration in the mixtures [1]. The IR spectra revealed no interaction occurred during the loading of oxaliplatin in pristine CNTs. The results are shown in Fig. 1.

SEM and TEM analysis

The prepared FA-CHI-FSWCNT-OXA-loaded complexes were found to be cylindrical and uniform in shape, as seen in SEM images. The Fig. 2a and b represent nanotubes with a size range of 1–300 nm. Figure 2a shows the pristine SWCNTs before loading the oxaliplatin, while Fig. 2b shows the drug after loading on modified SWCNT.

The TEM analysis of pristine and FA-CHI-FSWCNT-OXA is shown in Fig. 2. The TEM analysis clearly identified the difference in the size and morphology of the SWCNTs after drug loading. Figure 2c and

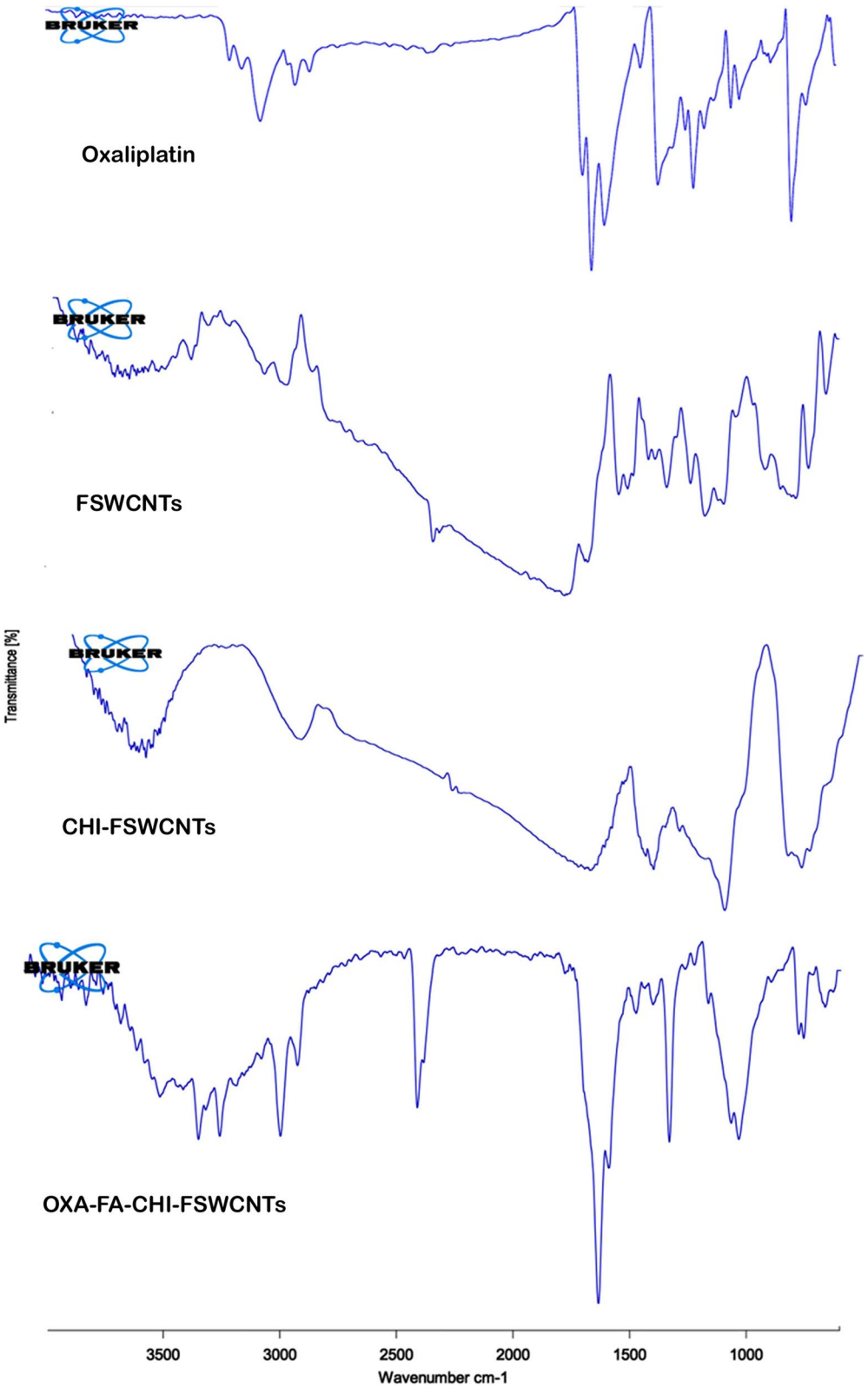

Fig. 1 FTIR spectra of oxaliplatin, FSWCNT, CHI-FSWCNT, and FA-CHI-FSWCNT-OXA

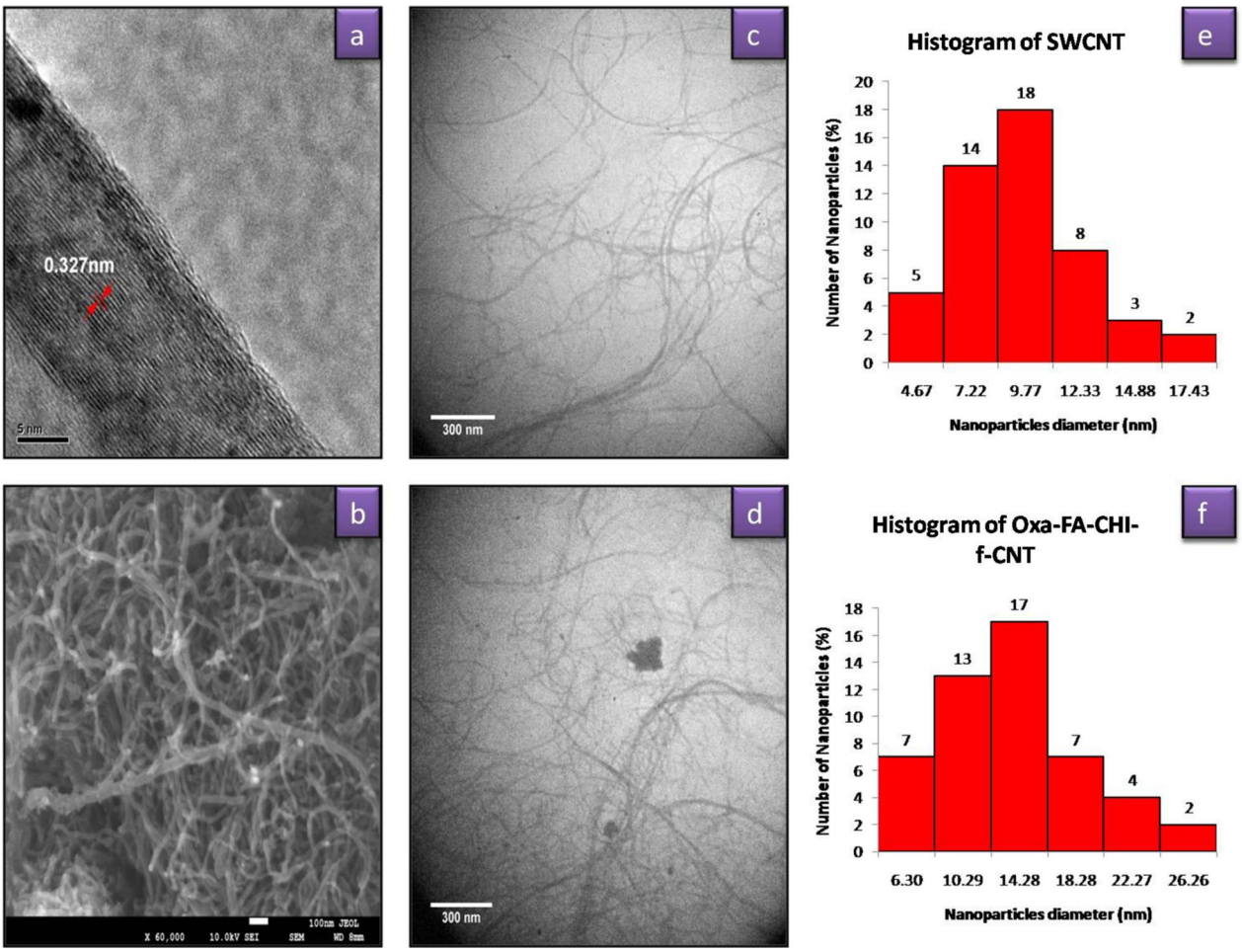

Fig. 2 SEM images **a** before and **b** after drug loading, TEM images **c** before and **d** after drug loading, and histogram of **e** before and **f** after drug loading

d show a change in the structure and morphology of pristine SWCNTs as chitosan, folic acid, and oxaliplatin were attached to the FSWCNTs before and after drug loading, respectively. The nanotube histogram, shown in Fig. 2e and f, revealed that the average particle size of SWCNTs before and after drug loading was 8.31 ± 3.24 nm and 11.57 ± 5.21 nm, respectively. The PDI values for the FSWCNTs and FA-CHI-FSWCNT-OXA were found to be 1.0387 and 1.0515, respectively.

X-Ray diffraction study

Figure 3 depicts the X-ray diffractogram of a FA-CHI-FSWCNT-OXA nanocomposite. The diffraction pattern revealed many characteristic peaks due to the crystalline nature of oxaliplatin and CNTs. FA-CHI-FSWCNT-OXA nanocomposite exhibited characteristic high-energy diffraction peaks at 2θ values between 3° and 38°, with a sharp and some narrow peaks at 23.22°, 24.32°, 25.75° and 36.11°.

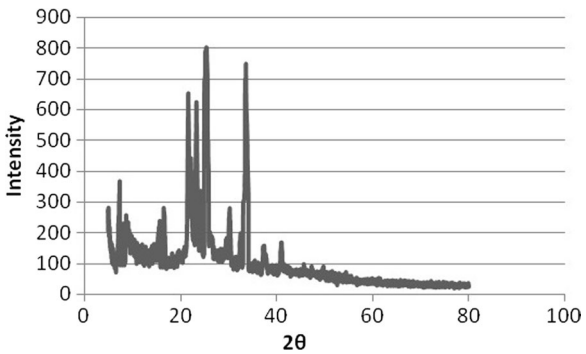

Fig. 3 X-ray diffractogram of FA-CHI-FSWCNT-OXA

Zeta potential and particle size analysis

Zeta potential studies were performed to study the variation in surface charge after modifications to CNTs. Plain SWCNTs exhibited negative zeta potential of − 27.1 mV (Fig. 4a), whereas FSWCNTs exhibited a more negative zeta potential (− 37.8 mV) because of the introduction of –COOH and –OH upon modification (Fig. 4b). When FSWCNTs were reacted with cationic (positively charged) chitosan, the zeta potential value becomes less negative (− 26.2 mV) (Fig. 4c). On the other hand, when anionic-charged oxaliplatin reacted with FA-CHI-FSWCNT, the zeta potential value was found to be more negative, i.e., − 31.6 mV (Fig. 4d). This corroborated the adhering of anionic oxaliplatin to FA-CHI-FSWCNTs via electrostatic and/or π-π stacking interactions [54–57]. The Z-average particle size of FA-CHI-FSWCNT-OXA was found to be 149.6 nm (Fig. 5a).

Differential scanning calorimeter (DSC)

DSC thermogram of FA-CHI-FSWCNT-OXA is depicted in Fig. 5b. The oxaliplatin-loaded FSWCNTs showed a prominent exothermic peak at 382.63°C, which corresponded to the melting transition temperature and decomposition of SWCNTs. A prominent endothermic peak signified that SWCNTs and oxaliplatin existed in a pure crystalline state. Also, it helped to confirm the stability, as compatibility among the drug, polymer, and CNTs helped providing stability to the preparation [3].

Thermo-gravimetric analysis (TGA)

FA-CHI-FSWCNT-OXA showed almost different weight loss patterns during the first stage in the range of 235–270 °C attributed to the degradation of oxaliplatin, whereas the second stage (360–380 °C) can be attributed to the decomposition of different structures of the newly formed polymeric network (Fig. 5c) [58].

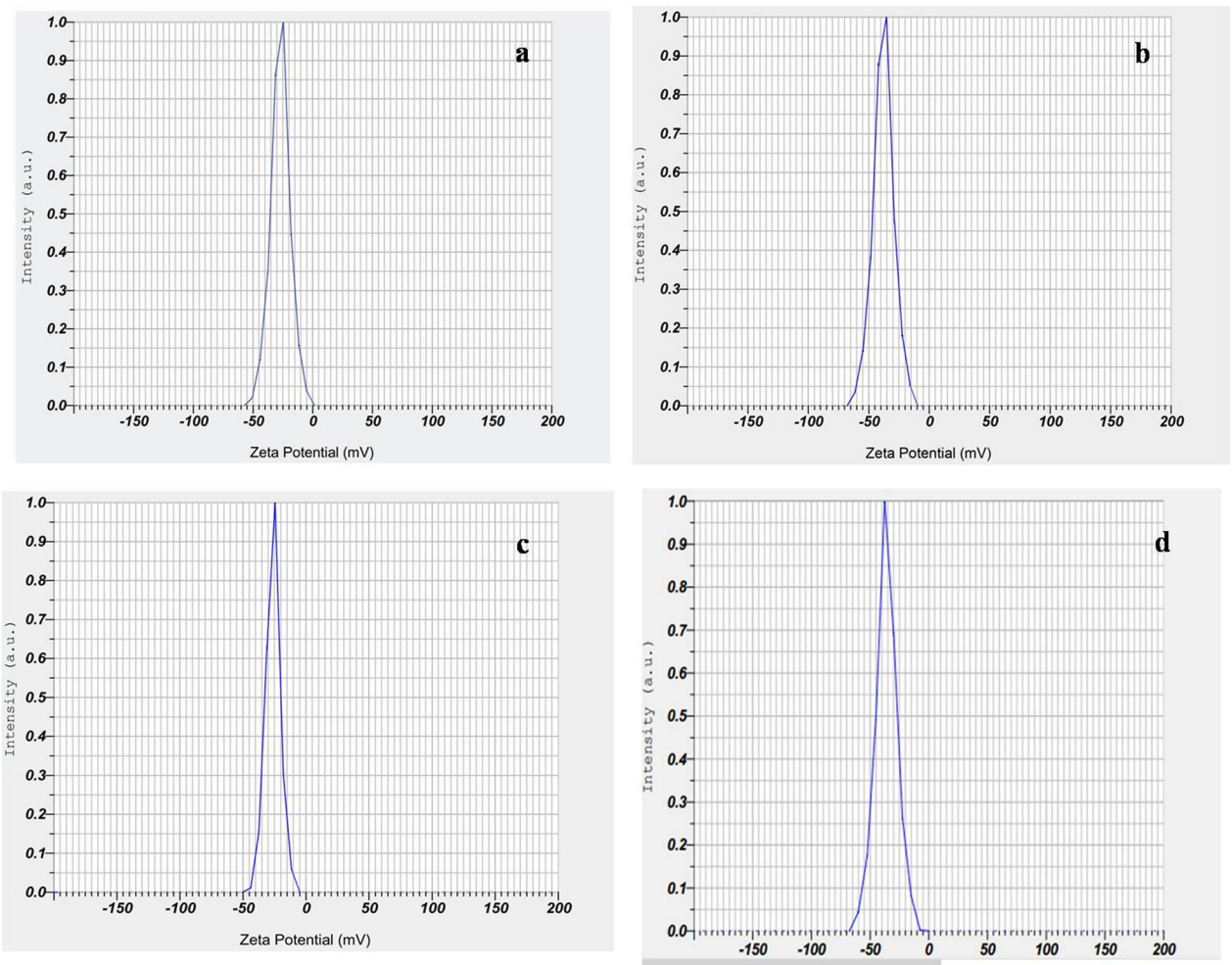

Fig. 4 Zeta potential of **a** SWCNT, **b** FSWCNT, **c** CHI-FSWCNT and **d** FA-CHI-FSWCNT-OXA

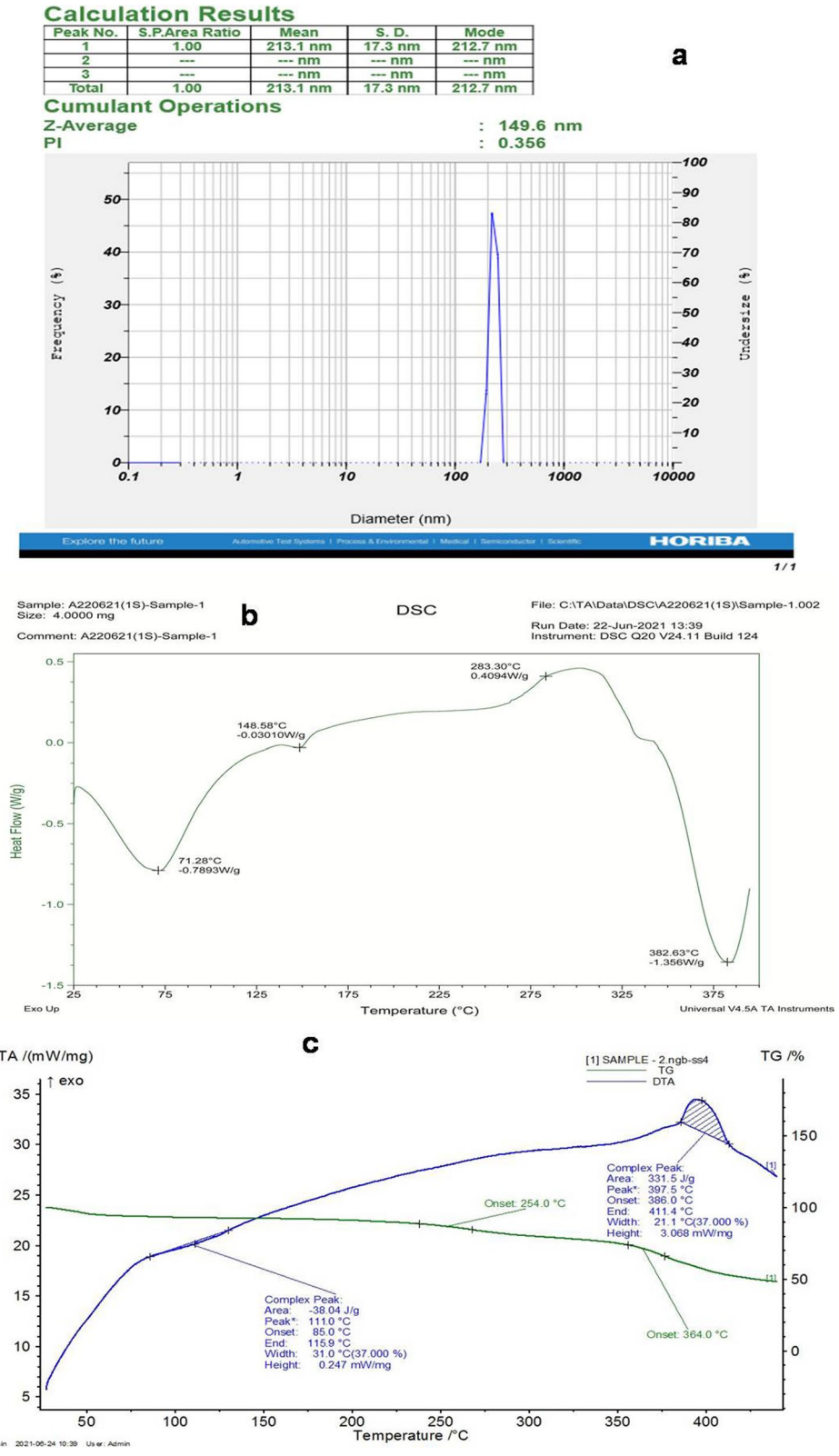

Fig. 5 **a** Particle size analysis, **b** DSC spectra and **c** TGA analysis of FA-CHI-FSWCNT-OXA

Drug entrapment efficiency (EE)

Oxaliplatin entrapment in the functionalized SWCNTs was found to be 93.43 ± 1.65%. Also, the attachment of chitosan rendered the nanotube aqueous soluble, and the attachment of drugs and other hydrophilic polymers to the nanotube was facilitated.

In vitro Oxaliplatin release studies

Graphical representation of oxaliplatin release from FA-CHI-FSWCNT-OXA nanocomposite is shown in Fig. 6b**.** In pH 7.4 buffer medium, 54.02 ± 1.43% oxaliplatin release was observed at 10 h, which was further increased to 94.73 ± 0.89% at the end of 24 h.

In vitro cytotoxicity study

FA-CHI-FSWCNT-OXA exhibited 92.35 ± 0.94% inhibition as compared to oxaliplatin, which showed 66.58 ± 0.38% inhibition of COLO320DM cells, revealed by MTT assay, whereas the results of SRB assay revealed that FA-CHI-FSWCNT-OXA and oxaliplatin inhibited viability of 91.22 ± 0.90% and 76.69 ± 0.52% COLO320DM cells, respectively.

As per the MTT and SRB assays, FA-CHI-FSWCNT-OXA showed 94.14 ± 1.12% and 87.51 ± 1.1% inhibition, whereas plain oxaliplatin exhibited 76.34 ± 0.95% and 72.78 ± 0.35% inhibition of HT29 cells, respectively. Significant difference was observed ($P < 0.05$) between

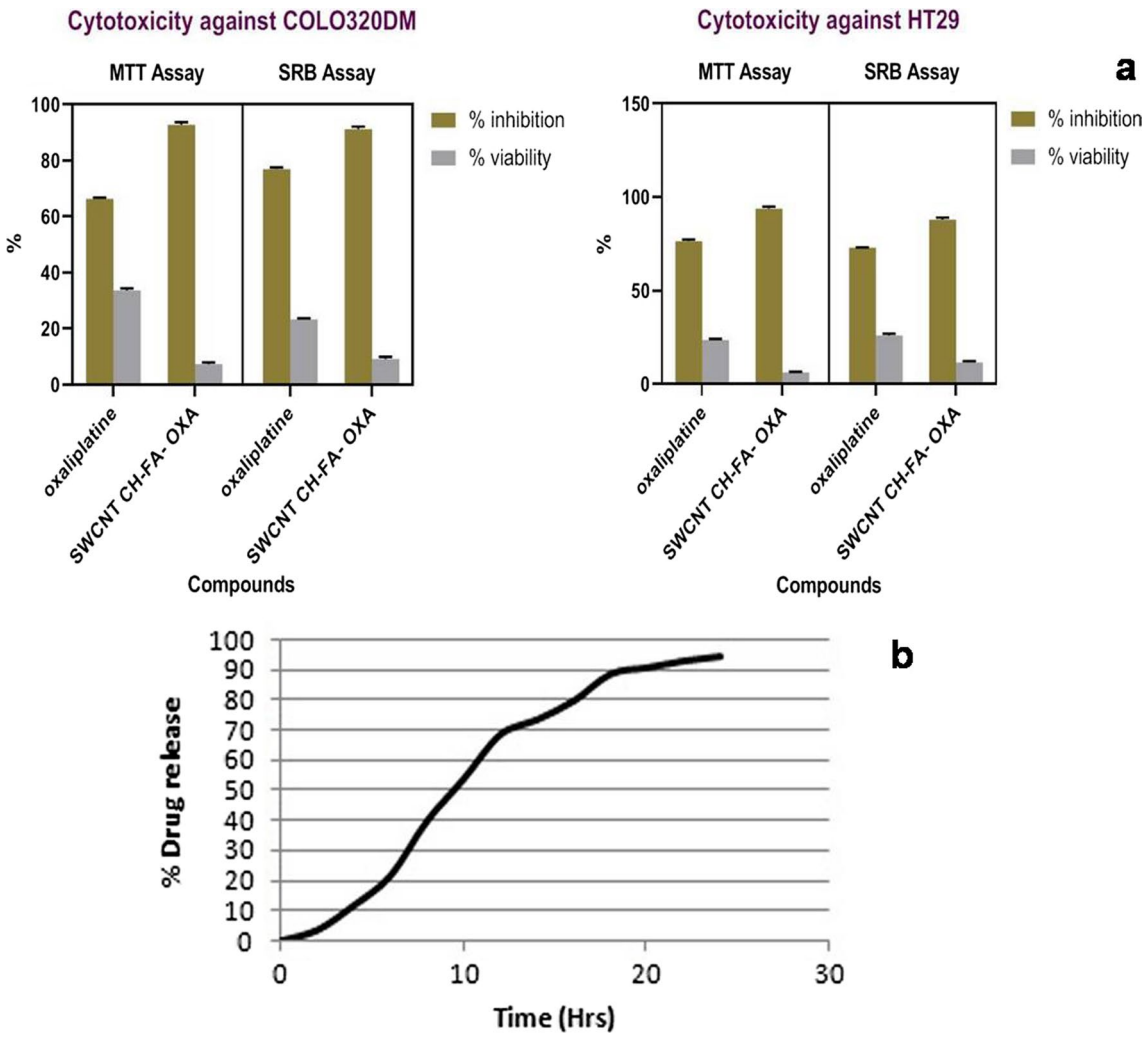

Fig. 6 **a** In vitro cytotoxicity results of FA-CHI-FSWCNT-OXA against COLO320 DM and HT29 cells by MTT and SRB assay **b** % drug release of oxaliplatin from FA-CHI-FSWCNT-OXA

Table 1 In vitro cytotoxicity of oxaliplatin and FA-CHI- FSWCNT-OXA against COLO320DM

Compound	% inhibition	% viability
In vitro cytotoxicity of oxaliplatin and FA-CHI- FSWCNT-OXA against COLO320DM		
MTT assay		
Oxaliplatin plain	66.58 ± 0.38	33.36 ± 0.74
FA-CHI-FSWCNT-OXA	92.36 ± 0.94***	7.2333 ± 0.64***
SRB assay		
Oxaliplatin plain	76.69 ± 0.52	23.3766 ± 0.44
FA-CHI-FSWCNT-OXA	91.22 ± 0.90***	9.2566 ± 0.74***
In vitro *cytotoxicity of oxaliplatin and FA-CHI- FSWCNT-OXA against HT29*		
MTT assay		
Oxaliplatin plain	76.34 ± 0.95	23.70 ± 0.74
FA-CHI- FSWCNT-OXA	94.14 ± 1.12***	6.35 ± 0.37***
SRB assay		
Oxaliplatin plain	72.78 ± 0.35	25.44 ± 1.04
FA-CHI- FSWCNT-OXA	87.51 ± 1.10***	11.64 ± 0.86***

All values are expressed as the mean ± the standard deviation ($n = 3$). The results are exposed as the mean values ± SEM. ***$P < 0.001$, ns—not significant when compared to respective control values by Student's *t* test

results of cell viabilities obtained by both assays after treatment with plain drug and FA-CHI-FSWCNT-OXA. This may be because of higher uptake of oxaliplatin by cells through FA-CHI-FSWCNT-OXA which could penetrate the cells and carry the oxaliplatin into cells [8]. Results of cytotoxicity against COLO320DM and HT29 are shown in Table 1 and Fig. 6a.

Apoptosis assay by flow cytometry

Several assays, such as signaling pathways and apoptosis, help to understand the anti-proliferative effects in a better manner. Thus, fluorescence-activated cell sorting (FACS) analysis was carried out for the selected cell lines. The flow cytometric Annexin V-FITC/PI assay for FA-CHI-FSWCNT-OXA exhibited a significant rise in the population of apoptotic cells compared to the control (Fig. 7). Early apoptosis of COLO320DM cells was noted to be 0.03% in control and 0.80% on FA-CHI-FSWCNT-OXA treatment, while the dead population of control and FA-CHI-FSWCNT-OXA-treated cells was found to be 0.38% and 10.3%, respectively. In HT29 cells dead population was found to be 14.8% as shown in Fig. 7.

Discussion

As a well-known fact, the conventional systems of drug delivery lack target specificity and therefore often fail to deliver the drug at the desired site in the desired concentrations, a shortcoming that can be successfully overcome by the use of CNTs. They possess little size and a relatively greater specific surface area, which offers them uniqueness and makes them a capable tool to achieve successful delivery of a variety of therapeutic molecules and diagnostics. Also, CNTs possess remarkable adsorption properties and get adsorbed on biological substrates. This property of CNTs offers them greater utility to be used as outstanding carriers in targeted systems of drug delivery, particularly in the case of cancer chemotherapy [59–61], which has reportedly increased the cell permeability in cancer cells. The carbon nanotube possesses enormous physicochemical properties, and it is possible to attach or load the drug along with a targeting agent and deliver it at a specific site to avoid drug exposure to the normal cells.

Some receptors, such as folate receptors (R-FA), are found to be overexpressed during the stages of cancer; thus, the substrate(s) that have affinity for such specific receptors can be used as targeting agents (folic acid) to deliver drugs at the specific site [62]. Thus, the toxic side effects due to the higher doses of the synthetic anticancer drugs can be minimized using this approach, and therefore, folic acid was anchored to CNTs in the proposed research. Moreover, chitosan-modified CNTs possesses a hydrophilic nature, which further increases the solubility of CNTs and facilitates its prompt excretion from the body. The carbon nanotubes with loading of anticancer drug within the size range of 1–300 nm exhibited better cell permeation as compared with pure drugs; this may become a novel approach for targeting cancerous cells.

Oxaliplatin belongs to the class of platinum-based antineoplastic therapeutics that is known to act by blocking the duplication of DNA. It exhibits a moderate effect against advanced colorectal cancer, possesses a problem of rapid elimination (half-life: 10–25 min), and also exhibits severe side effects. In the case of anticancer drugs, it is often considered beneficial if the drug delivery system precisely delivers the drug at the targeted (tumor) site, thereby minimizing the possible side effects of the drug on the normal cells. Because of the aforementioned unique properties, CNTs can be imbued with target specificity. Therefore, an attempt was made to develop a system that comprised oxaliplatin loaded on the CNTs.

The shifting of surface charge values from negative to positive indicated that chemical bonds present in oxaliplatin helped to prevail over the negative charge of the carboxylic group present on the surface of SWCNTs. It provides functionality by allowing molecules to be bound to the surface of SWCNT by covalent bonds [63]. The reason for preferring the use of FSWCNTs in the present study is that plain CNTs possess less dispersive abilities and also impart lowered stability to facilitate drug (oxaliplatin) loading. Also, one more possibility may

Apoptosis study by Flow cytometer

Table - Apoptosis assay by flow cytometer against COLO320DM and HT29 cell lines

Cell line	Live	Early Apoptosis	Late Apoptosis	Dead
Control	99.5%	0.03%	0.06%	0.38%
F-SWCNT-OXA-CHA-FA against COLO320DM	78.4%	0.80%	10.5%	10.3%
F-SWCNT-OXA-CHA-FA against HT29	70.0%	0.00%	15.2%	14.8%

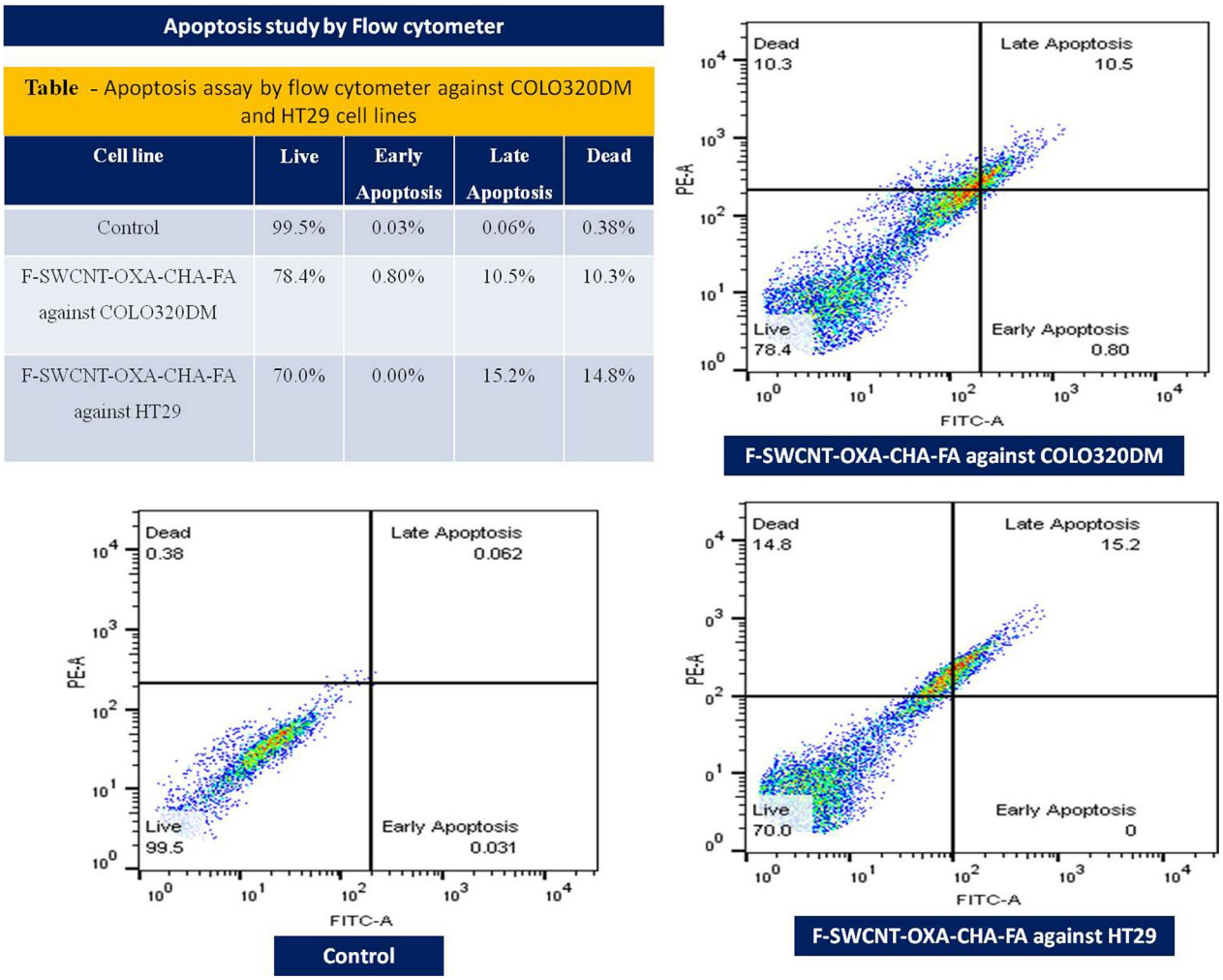

Fig. 7 Apoptosis study of FA-CHI-FSWCNT-OXA against COLO320 DM and HT29 cells

exist, which is an interaction of oxaliplatin with the carboxylic group of F-CNTs, which causes the liberation of H_2O, as shown in the IR spectrum of oxaliplatin-loaded FSWCNT.

The SEM and XRD analyses also revealed a crystalline nanoscale SWCNT composite. The cumulative percentage of release of oxaliplatin was recorded at 94.73 ± 0.90% at the end of 24 h, and it was achieved in a controlled manner. The EE of SWCNTs was found to be 93.43 ± 1.65% which is attributed to the hydrophilic characteristics imparted owing to chitosan loading on FSWCNT.

The tools FTIR, SEM, and XRD investigated the morphology as well as the structural features of oxaliplatin and modified CNTs. More than 90% of oxaliplatin was entrapped in SWCNTs. Interestingly, FSWCNTs loaded with oxaliplatin exhibited controlled release of the drug for about 24 h, in contrast to the pure drug, which proves the utility of the system to deliver a drug to a specific desired site in a controlled manner. In vitro anticancer studies revealed that oxaliplatin-loaded FSWCNTs inhibited the COLO320DM cell line by 92.35 ± 0.94% when compared to pure oxaliplatin in MTT and SRB assays. In case of HT29 cell lines, by MTT and SRB assays, the drug-loaded FSWCNTs exhibited percentage inhibitions of 94.14 ± 1.12% and 87.51 ± 1.1%, respectively. In both the assay methods, it was found that the percent inhibition of the SWCNT-loaded system exhibited better anticancer potential against cell lines in vitro, possibly owing to the effective cell-permeable property of the CNTs [54].

In the present research, we have attempted to study the comparative evaluation of anticancer activity exhibited by oxaliplatin-loaded FSWCNTs and pure oxaliplatin using two different in vitro assay methods. Still further scope exists for undertaking studies on the

exterior coating of CNTs with suitable biocompatible polymers such as polysaccharides, polyethylene glycol, and proteins, which may probably improve the utility of CNTs as drug carriers. Our results and observations may likely prove to be beneficial for the aforesaid theme.

Conclusion

From the results obtained, the developed system of FA-CHI-FSWCNT-OXA was found to be more efficient as compared to oxaliplatin. The developed system of SWCNTs loaded with oxaliplatin showed better in vitro cytotoxicity against COLO320DM and HT29 cell lines than the oxaliplatin. Also, flow cytometry showed better results for the developed system against COLO320DM and HT29 cell lines as compared to control. The physical and chemical properties like TGA, DSC, particle size, and SEM and TEM studies exhibited acceptable results. We therefore, conclude that the developed system is more competent than using pure anticancer agents to minimize the possible side effect(s) of these drugs. Furthermore, a suitable in vivo model is required to assess the FA-CHI-FSWCNTs-OXA's site-specific action.

Abbreviations

CHI	Chitosan
OXA	Oxaliplatin
FA	Folic acid
CNT	Carbon nanotube
FA-CHI-FSWCNT-OXA	Oxaliplatin to the functionalized nanotube
CRC	Colorectal carcinoma
SWCNTs	Single-walled carbon nanotubes
MWNTs	Multi-walled carbon nanotubes
PTT	Photothermal treatment
PDT	Photodynamic therapy
NPs	Nanoparticles
EE	Entrapment efficiency

Author contributions

Investigation was done by Dheeraj Randive, Kiran Shejawal, and Sandeep Patil. Visualization was done by Dheeraj Randive, Kiran Shejawal, and Sandeep Patil. Data curation was done by Dheeraj Randive and Mangesh Bhutkar. Funding acquisition was done by Dheeraj Randive. Writing—Original Draft was done by Dheeraj Randive, Kiran Shejawal, and Sandeep Patil. Formal analysis was carried out by Kiran Shejawal and Mangesh Bhutkar. Conceptualization was done by Somnath Bhinge and Sameer Nadaf. Validation was done by Somnath Bhinge, Mangesh Bhutkar, and Namdeo Jadhav. Supervision was done by Somnath Bhinge, Namdeo Jadhav, and Sameer Nadaf. Writing—Review and Editing were done by Somnath Bhinge, Namdeo Jadhav, and Sameer Nadaf. Methodology was done by Namdeo Jadhav and Sameer Nadaf. Software was done by Sameer Nadaf. Project administration was done by Sameer Nadaf. Resources were carried out by Sandeep Patil.

Funding

The authors have received a Research Grant (SU/C& U.D. Section/83/579 and 239) from the Board of College and University Department of SU, Kolhapur, under the Research Initiation Scheme (RIS-2017). We are therefore extremely thankful and highly acknowledge the help extended by BCUD and Shivaji University, Kolhapur (M.S.), India.

Availability of data and materials

The data that support the findings of this study are available from the corresponding author, upon reasonable request.

Declarations

Ethics approval and consent to participate

Not applicable.

Competing interests

The authors declare that they have no competing interests.

Received: 19 August 2023 Accepted: 10 October 2023
Published online: 23 October 2023

References

1. Jain A, Jain SK, Ganesh N, Barve J, Beg AM (2010) Design and development of ligand-appended polysaccharidic nanoparticles for the delivery of oxaliplatin in colorectal cancer. Nanomedicine 6(1):179–190. https://doi.org/10.1016/j.nano.2009.03.002
2. Yang C, Liu HZ, Fu ZX, Lu WD (2011) Oxaliplatin long-circulating liposomes improved therapeutic index of colorectal carcinoma. BMC Biotechnol 11:21. https://doi.org/10.1186/1472-6750-11-21
3. Tummala S, Gowthamarajan K, Satish Kumar MN, Wadhwani A (2016) Oxaliplatin immuno hybrid nanoparticles for active targeting: an approach for enhanced apoptotic activity and drug delivery to colorectal tumors. Drug Deliv 23(5):1773–1787. https://doi.org/10.3109/10717544.2015.1084400
4. Buyana B, Naki T, Alven S, Aderibigbe BA (2022) Nanoparticles loaded with platinum drugs for colorectal cancer therapy. Int J Mol Sci 23(19):11261. https://doi.org/10.3390/ijms231911261
5. Li L, Ahmed B, Mehta K, Kurzrock R (2007) Liposomal curcumin with and without oxaliplatin: effects on cell growth, apoptosis, and angiogenesis in colorectal cancer. Mol Cancer Ther 6(4):1276–1282. https://doi.org/10.1158/1535-7163.MCT-06-0556
6. Virag P, Fischer-Fodor E, Perde-Schrepler M, Brie I, Tatomir C, Balacescu L, Berindan-Neagoe I, Victor B, Balacescu O (2013) Oxaliplatin induces different cellular and molecular chemoresistance patterns in colorectal cancer cell lines of identical origins. BMC Genom 14:480. https://doi.org/10.1186/1471-2164-14-480
7. O'Dwyer PJ, Johnson SW (2003) Current status of oxaliplatin in colorectal cancer. Semin Oncol 30(3 Suppl 6):78–87. https://doi.org/10.1016/s0093-7754(03)00215-x
8. Wu L, Man C, Wang H, Lu X, Ma Q, Cai Y, Ma W (2013) PEGylated multi-walled carbon nanotubes for encapsulation and sustained release of oxaliplatin. Pharm Res 30(2):412–423. https://doi.org/10.1007/s11095-012-0883-5
9. Brown SD, Nativo P, Smith JA, Stirling D, Edwards PR, Venugopal B, Flint DJ, Plumb JA, Graham D, Wheate NJ (2010) Gold nanoparticles for the improved anticancer drug delivery of the active component of oxaliplatin. J Am Chem Soc 132(13):4678–4684. https://doi.org/10.1021/ja908117a
10. Haller DG, Tabernero J, Maroun J, de Braud F, Price T, Van Cutsem E, Hill M, Gilberg F, Rittweger K, Schmoll HJ (2011) Capecitabine plus oxaliplatin compared with fluorouracil and folinic acid as adjuvant therapy for stage III colon cancer. J Clin Oncol 29(11):1465–1471. https://doi.org/10.1200/JCO.2010.33.6297
11. Li B, Meng Z, Li Q, Huang X, Kang Z, Dong H, Chen J, Sun J, Dong Y, Li J, Jia X, Sessler JL, Meng Q, Li C (2017) A pH responsive complexation-based drug delivery system for oxaliplatin. Chem Sci 8(6):4458–4464. https://doi.org/10.1039/c7sc01438d
12. Branca JJV, Carrino D, Gulisano M, Ghelardini C, Di Cesare ML, Pacini A (2021) Oxaliplatin-induced neuropathy: genetic and epigenetic profile to better understand how to ameliorate this side effect. Front Mol Biosci 8:643824. https://doi.org/10.3389/fmolb.2021.643824

13. Cavaletti G, Marmiroli P (2020) Management of oxaliplatin-induced peripheral sensory neuropathy. Cancers 12(6):1370. https://doi.org/10.3390/cancers12061370
14. Lila AS, Kiwada H, Ishida T (2014) Selective delivery of oxaliplatin to tumor tissue by nanocarrier system enhances overall therapeutic efficacy of the encapsulated oxaliplatin. Biol Pharm Bull 37(2):206–211. https://doi.org/10.1248/bpb.b13-00540
15. Zare H, Ahmadi S, Ghasemi A, Ghanbari M, Rabiee N (2021) Carbon nanotubes: smart drug/gene delivery carriers [published correction appears in Int J Nanomedicine. 16:7283–7284]. Int J Nanomed 16:1681–1706. https://doi.org/10.2147/IJN.S299448
16. Sharifi J, Fayazfar H (2021) Highly sensitive determination of doxorubicin hydrochloride antitumor agent via a carbon nanotube/gold nanoparticle based nanocomposite biosensor. Bioelectrochemistry 139:107741. https://doi.org/10.1016/j.bioelechem.2021.107741
17. Sharifianjazi F, Jafari Rad A, Bakhtiari A, Niazvand F, Esmaeilkhanian A, Bazli L, Abniki M, Irani M, Moghanian A (2021) Biosensors and nanotechnology for cancer diagnosis (lung and bronchus, breast, prostate, and colon): a systematic review. Biomed Mater. https://doi.org/10.1088/1748-605X/ac41fd
18. Geetha Bai R, Muthoosamy K, Tuvikene R, Nay Ming H, Manickam S (2021) Highly sensitive electrochemical biosensor using folic acid-modified reduced graphene oxide for the detection of cancer biomarker. Nanomaterials 11(5):1272. https://doi.org/10.3390/nano11051272
19. Singh R, Deshmukh R (2022) Carbon nanotube as an emerging theranostic tool for oncology. J Drug Deliv Sci Technol 74:103586. https://doi.org/10.1016/j.jddst.2022.103586
20. Dineshkumar B, Krishnakumar K, Bhatt AR, Paul D, Cherian J, John A (2015) Single-walled and multi-walled carbon nanotubes based drug delivery system: Cancer therapy: a review. Indian J Cancer 52(3):262–264. https://doi.org/10.4103/0019-509X.176720
21. Singh R, Kumar S (2022) Cancer targeting and diagnosis: recent trends with carbon nanotubes. Nanomaterials 12(13):2283. https://doi.org/10.3390/nano12132283
22. Murjani BO, Kadu PS, Bansod M, Vaidya SS, Yadav MD (2022) Carbon nanotubes in biomedical applications: current status, promises, and challenges. Carbon Lett 32:1207–1226. https://doi.org/10.1007/s42823-022-00364-4
23. Liu Z, Tabakman S, Welsher K, Dai H (2009) Carbon nanotubes in biology and medicine: In vitro and in vivo detection, imaging and drug delivery. Nano Res 2(2):85–120. https://doi.org/10.1007/s12274-009-9009-8
24. Zaboli M, Raissi H, Zaboli M (2022) Investigation of nanotubes as the smart carriers for targeted delivery of mercaptopurine anticancer drug. J Biomol Struct Dyn 40(10):4579–4592. https://doi.org/10.1080/07391102.2020.1860823
25. Sargazi S, Er S, Mobashar A, Gelen SS, Rahdar A, Ebrahimi N, Hosseinikhah SM, Bilal M, Kyzas GZ (2022) Aptamer-conjugated carbon-based nanomaterials for cancer and bacteria theranostics: a review. Chem Biol Interact 361:109964. https://doi.org/10.1016/j.cbi.2022.109964
26. Murugesan R, Raman S (2022) Recent trends in carbon nanotubes based prostate cancer therapy: a biomedical hybrid for diagnosis and treatment. Curr Drug Deliv 19(2):229–237. https://doi.org/10.2174/1567201818666210224101456
27. Bura C, Mocan T, Grapa C, Mocan L (2022) Carbon nanotubes-based assays for cancer detection and screening. Pharmaceutics 14(4):781. https://doi.org/10.3390/pharmaceutics14040781
28. Elhissi AM, Ahmed W, Hassan IU, Dhanak VR, D'Emanuele A (2012) Carbon nanotubes in cancer therapy and drug delivery. J Drug Deliv 2012:837327. https://doi.org/10.1155/2012/837327
29. Huang H, Yang X (2004) Synthesis of polysaccharide-stabilized gold and silver nanoparticles: a green method. Carbohydr Res 339(15):2627–2631. https://doi.org/10.1016/j.carres.2004.08.005
30. Huang H, Yuan Q, Yang X (2005) Morphology study of gold-chitosan nanocomposites. J Colloid Interface Sci 282(1):26–31. https://doi.org/10.1016/j.jcis.2004.08.063
31. Feng JJ, Zhao G, Xu JJ, Chen HY (2005) Direct electrochemistry and electrocatalysis of heme proteins immobilized on gold nanoparticles stabilized by chitosan. Anal Biochem 342(2):280–286. https://doi.org/10.1016/j.ab.2005.04.040
32. Tan WB, Zhang Y (2005) Surface modification of gold and quantum dot nanoparticles with chitosan for bioapplications. J Biomed Mater Res A 75(1):56–62. https://doi.org/10.1002/jbm.a.30410
33. Agnihotri SA, Mallikarjuna NN, Aminabhavi TM (2004) Recent advances on chitosan-based micro- and nanoparticles in drug delivery. J Control Release 100(1):5–28. https://doi.org/10.1016/j.jconrel.2004.08.010
34. Kim TH, Park IK, Nah JW, Choi YJ, Cho CS (2004) Galactosylated chitosan/DNA nanoparticles prepared using water-soluble chitosan as a gene carrier. Biomaterials 25(17):3783–3792. https://doi.org/10.1016/j.biomaterials.2003.10.063
35. Janes KA, Fresneau MP, Marazuela A, Fabra A, Alonso MJ (2001) Chitosan nanoparticles as delivery systems for doxorubicin. J Control Release 73(2–3):255–267. https://doi.org/10.1016/s0168-3659(01)00294-2
36. Mansouri S, Cuie Y, Winnik F, Shi Q, Lavigne P, Benderdour M, Beaumont E, Fernandes JC (2006) Characterization of folate-chitosan-DNA nanoparticles for gene therapy. Biomaterials 27(9):2060–2065. https://doi.org/10.1016/j.biomaterials.2005.09.020
37. Tsai P-A, Kuo H-Y, Chiu W-M, Wu J-H (2013) Purification and functionalization of single-walled carbon nanotubes through different treatment procedures. J Nano Mat 2013:937697. https://doi.org/10.1155/2013/937697
38. Huang H, Yuan Q, Shah JS, Misra RD (2011) A new family of folate-decorated and carbon nanotube-mediated drug delivery system: synthesis and drug delivery response. Adv Drug Deliv Rev 63(14–15):1332–1339. https://doi.org/10.1016/j.addr.2011.04.001
39. Sudimack J, Lee RJ (2000) Targeted drug delivery via the folate receptor. Adv Drug Deliv Rev 41(2):147–162. https://doi.org/10.1016/s0169-409x(99)00062-9
40. Li H, Zhang N, Hao Y, Wang Y, Jia S, Zhang H, Zhang Y, Zhang Z (2014) Formulation of curcumin delivery with functionalized single-walled carbon nanotubes: characteristics and anticancer effects in vitro. Drug Deliv 21(5):379–387. https://doi.org/10.3109/10717544.2013.848246
41. Randive DS, Bhinge SD, Bhutkar MA, Jadhav NR, Shirsat M (2023) Single walled Carbon nanotube: Chitosan conjugate for sustained ophthalmic delivery of Ciprofloxacin from ointment; its evaluation and in vivo eye irritation study. Sep Sci Technol 58(4):775–788. https://doi.org/10.1080/01496395.2022.2160349
42. Zhang X, Meng L, Lu Q, Fei Z, Dyson PJ (2009) Targeted delivery and controlled release of doxorubicin to cancer cells using modified single wall carbon nanotubes. Biomaterials 30(30):6041–6047. https://doi.org/10.1016/j.biomaterials.2009.07.025
43. Vakhariya RR, Salunkhe VR, Randive DS, Bhutkar MA, Bhinge SD (2019) Design, development and optimization of ramipril solid lipid nanoparticles using solvent emulsification and evaporation method. Nanosci Nanotechnol Asia 11:42–52. https://doi.org/10.2174/2210681206966191204113659
44. Zeng H, Gao C, Wang Y, Watts PCP, Kong H, Cui X, Yan D (2006) In situ polymerization approach to multiwalled carbon nanotubes-reinforced nylon 1010 composites: Mechanical properties and crystallization behavior. Polymer 47:113–122. https://doi.org/10.1016/j.polymer.2005.11.009
45. Kamble RV, Bhinge SD, Mohite SK, Randive DS, Bhutkar MA (2021) In vitro targeting and selective killing of mcf-7 and colo320dm cells by 5-fluorouracil anchored to carboxylated SWCNTs and MWCNTs. J Mater Sci Mater Med 32(6):71. https://doi.org/10.1007/s10856-021-06540-8
46. Peng H, Alemany LB, Margrave JL, Khabashesku VN (2003) Sidewall carboxylic acid functionalization of single-walled carbon nanotubes. J Am Chem Soc 125(49):15174–15182. https://doi.org/10.1021/ja037746s
47. Sobh RA, Nasr HES, Mohamed WS (2019) Formulation and in vitro characterization of anticancer drugs encapsulated chitosan/multi-walled carbon nanotube nanocomposites. J Appl Pharm Sci 9:32–40. https://doi.org/10.7324/JAPS.2019.90805
48. Mosmann T (1983) Rapid colorimetric assay for cellular growth and survival: application to proliferation and cytotoxicity assays. J Immunol Methods 65(1–2):55–63. https://doi.org/10.1039/c6ra17788c
49. Shejawal KP, Randive DS, Bhinge SD, Bhutkar MA, Wadkar GH, Jadhav NR (2020) Green synthesis of silver and iron nanoparticles of isolated proanthocyanidin: its characterization, antioxidant, antimicrobial, and cytotoxic activities against COLO320DM and HT29. J Genet Eng Biotechnol 18(1):43. https://doi.org/10.1186/s43141-020-00058-2
50. Chavan R, Bhinge SD, Bhutkar MA, Randive SD, Wadkar GH (2021) Characterization, antioxidant, antimicrobial and cytotoxic activities of green

synthesized silver and iron nanoparticles using alcoholic Blumea eriantha DC plant extract. Mater Today Commun 24:1–2. https://doi.org/10.1016/j.mtcomm.2020.101320
51. Randive DS, Shejawal KP, Bhinge SD, Bhutkar MA, Patil PD, Jadhav NR, Patil SB (2020) Green synthesis of gold nanoparticles of isolated citrus bioflavonoid from orange: Characterization and in vitro cytotoxicity against colon cancer cell lines colo 320DM and Ht29. Indian Drugs 57:61–69
52. Shejawal KP, Randive DS, Bhinge SD, Bhutkar MA, Todkar SS, Mulla AS, Jadhav NR (2021) Green synthesis of silver, iron and gold nanoparticles of lycopene extracted from tomato: their characterization and cytotoxicity against COLO320DM, HT29 and Hella cell. J Mater Sci Mater Med 32(2):19. https://doi.org/10.1007/s10856-021-06489-8
53. Shejawal KP, Randive DS, Bhinge SD, Bhutkar MA, Wadkar GH, Todkar SS, Mohite SK (2021) Functionalized carbon nanotube for colon - targeted delivery of isolated lycopene in colorectal cancer : In vitro cytotoxicity and in vivo roentgenographic study. J Mater Res 36:4894–4907. https://doi.org/10.1557/s43578-021-00431-y
54. Singh N, Sachdev A, Gopinath P (2018) Polysaccharide functionalized single walled carbon nanotubes as nanocarriers for delivery of curcumin in lung cancer cells. J Nanosci Nanotechnol 18(3):1534–1541. https://doi.org/10.1166/jnn.2018.14222
55. Arya N, Arora A, Vasu KS, Sood AK, Katti DS (2013) Combination of single walled carbon nanotubes/graphene oxide with paclitaxel: a reactive oxygen species mediated synergism for treatment of lung cancer. Nanoscale 5(7):2818–2829. https://doi.org/10.1039/c3nr33190c
56. Rezwan K, Studart AR, Vörös J, Gauckler LJ (2005) Change of zeta potential of biocompatible colloidal oxide particles upon adsorption of bovine serum albumin and lysozyme. J Phys Chem B 109(30):14469–14474. https://doi.org/10.1021/jp050528w
57. Zhang Y, Ali SF, Dervishi E, Xu Y, Li Z, Casciano D, Biris AS (2010) Cytotoxicity effects of graphene and single-wall carbon nanotubes in neural phaeochromocytoma-derived PC12 cells. ACS Nano 4(6):3181–3186. https://doi.org/10.1021/nn1007176
58. Ullah K, Ali Khan S, Murtaza G, Sohail M, Azizullah MA, Afzal A (2019) Gelatin-based hydrogels as potential biomaterials for colonic delivery of oxaliplatin. Int J Pharm 556:236–245. https://doi.org/10.1016/j.ijpharm.2018.12.020
59. Son KH, Hong JH, Lee JW (2016) Carbon nanotubes as cancer therapeutic carriers and mediators. Int J Nanomed 11:5163–5185. https://doi.org/10.2147/IJN.S112660
60. Oberdörster E (2004) Manufactured nanomaterials (fullerenes, C60) induce oxidative stress in the brain of juvenile largemouth bass. Environ Health Perspect 112(10):1058–1062. https://doi.org/10.1289/ehp.7021
61. Bosi S, Da Ros T, Spalluto G, Prato M (2003) Fullerene derivatives: an attractive tool for biological applications. Eur J Med Chem 38(11–12):913–923. https://doi.org/10.1016/j.ejmech.2003.09.005
62. Randive DS, Gavade AS, Shejawal KP, Bhutkar MA, Bhinge SD, Jadhav NR (2021) Colon targeted dosage form of Capecitabine using folic acid anchored modified carbon nanotube: in vitro cytotoxicity, apoptosis and in vivo roentgenographic study. Drug Dev Ind Pharm 47(9):1401–1412. https://doi.org/10.1080/03639045.2021.1994988
63. Kazemi-Beydokhti A, Zeinali Heris S, Jaafari MR (2016) Investigation of different methods for cisplatin loading using single-walled carbon nanotube. Chem Eng Res Des 112:56–63. https://doi.org/10.1016/j.cherd.2016.06.006

Publisher's Note